PERMAFROST AND PERIGLACIAL PROCESSES
Permafrost and Periglac. Process. (2015)
Published online in Wiley Online Library
(wileyonlinelibrary.com) DOI: 10.1002/ppp.1878

Molards and Their Relation to Landslides Involving Permafrost Failure

*Juan Pablo Milana**

CONICET and the Universidad Nacional de San Juan, InGeo-FCEFyN, San Juan, Argentina

ABSTRACT

Molards are conical-shaped, often symmetrical debris mounds with a distinctive radial grain size gradation, which were first named in the Alps over 100 years ago. Historically, these landforms did not receive much academic attention as they were rarely observed. Today, six different genetic hypotheses can be applied to molards, and the most recent has suggested a link to permafrost failure. The aim of this research was to test the hypothesis that molards result from the failure of permafrost-bearing ground and subsequent thawing of the frozen debris boulders. This hypothesis is tested by: (1) reviewing the known global distribution of molard-bearing mass movements with respect to permafrost distribution; (2) investigating a landslide in the Andes of Argentina that unequivocally relates to permafrost failure; (3) describing and interpreting the external and internal structure of molards, applying sedimentary transport concepts; and (4) reproducing molards by laboratory simulation. The results show that, with few exceptions, molards are produced by melt-out of ground ice in permafrost blocks. In particular, a permafrost source of the mass flow is more certain for landslide deposits that are densely populated by molards. This study serves to reappraise the presence of molards as they could be used to track ground ice loss and potential permafrost degradation in mountainous areas and hence climate change. Copyright © 2015 John Wiley & Sons, Ltd.

KEY WORDS: molards; permafrost; landslides; climate change; natural hazards

INTRODUCTION

Molards are conical-shaped debris mounds, with a distinctive radial inward and vertical fining upward gradation in grain size, and a structure that rapidly evolves due to their inherent instability. Molards are often perfectly symmetrical, although their shape varies widely, including spiky symmetrical cones, asymmetrical cones and a gradation from a cone to a semi-sphere. Molards have been described as having a grain size finer (sandier) than the associated landslide debris but with a coarser-grained (breccia) core, leading to the use of terms such as bimodality (Cassie *et al.,* 1988) or xenolithological (Shreve, 1966) to describe them. Molards have been recognised, described and interpreted for more than a century (McConnell and Brock, 1904), but their documentation has been rare and they are seldom described in the literature. According to Goguel and Pachoud (1972), the term molard was coined in the Alps more than 100 years ago, but today is almost abandoned due to the rarity of this landform. Molards have always been described as elements of landslides and avalanches in glacial and periglacial environments (Shreve, 1968; Cassie *et al*., 1988; Brideau *et al.*, 2010). Their origin has long been debated, and recently they have been attributed, potentially, to permafrost thaw, although their linkage to permafrost and/or periglacial processes has only been suggested incidentally (Brideau *et al.*, 2010).

This paper presents new data collected on molards and discusses models for their origin. Its aim is to demonstrate a link between molards and the failure of mountain permafrost debris. It suggests that given the relatively high proportion of molards in the arid Andes (four occurrences within a 100 km segment of the Andes, see Table 1) that these failures may relate to a progressive loss of ice caused by the century-long drying out of the Andes (Rutllant and Fuenzalida, 1991; Minetti and Vargas, 1998; Rivera *et al*., 2000; Luckman and Villalba, 2001; Minetti *et al.*, 2003; Intergovernmental Panel on Climate Change (IPCC), 2007; Vuille and Milana, 2007). In many cases, this could suggest the origin of a landslide or other mass-wasting processes and thus serves as an indicator of possible climate change should molards be observed more frequently. The hypothesis is tested that molards result from the failure of permafrost-bearing ground and subsequent thawing of the frozen mass movement debris.

*Correspondence to: J. P. Milana, CONICET and the Universidad Nacional de San Juan, InGeo-FCEFyN, Av. I. de la Roza y Meglioli, 5401 Rivadavia, San Juan, Argentina. E-mail: jpmilana@gmail.com

Received 29 July 2014
Revised 13 August 2015
Accepted 4 September 2015

Table 1 Non-exhaustive record of molard-bearing landslides and characteristics of these landslides.

Landslide name (source)	Year	Latitude	Longitude	Alt.pf	Alt.max	Alt.min	H (m)	L (m)	La (m)	Fb (°)
Frank (Cassie *et al*., 1988)	1903	49° 35.6′N	114° 22.9′W	2100	2030	1310	720	3170	2018	12.8
Khait (Evans *et al*., 2009)	1949	39° 11.1'N	70° 52.6'E	2900	2991	1570	1421	7410	5136	10.9
Sherman (Shreve, 1966; Marangunic and Bull, 1968)	1964	60° 32.9'N	145° 11.8'W	500	980	230	750	5800	4600	7.4
Little Salmon Lake (Brideau *et al.*, 2010)	2008	62° 10.1'N	134° 36.7'W	600	1065	550	515	2050	1226	14.1
Pink Mountain (Geertsema *et al.*, 2006)	2002	57° 2.5'N	122° 53.7'W	1000	1460	1010	450	2000	1280	12.7
Yiyong River (Qiang *et al*., 2012)	2000	30° 10.8'N	94° 56.5'E	4000	5520	2188	3332	10000	4669	18.4
Sale Mountain (Zhang *et al*., 2002)	1983	35° 33.7'N	103° 35.2'E	3300	2283	1985	298	1600	1123	10.6
Seit (Strom and Abdrakhmatov, 2009)	??	42° 5.8'N	74° 8.3'E	2500	3280	2120	1160	3180	1324	20.1
Erizos South (this paper)	??	31° 42.4'S	70° 16.6'W	3500	4480	3040	1440	3400	1096	23.0
San Lorenzo (this paper)	??	30° 15.4'S	69° 49.7'W	4200	5000	4300	700	1655	535	22.9
Altares West (this paper)	??	31° 30.5'S	70° 32.1'W	3600	4280	3260	1020	5880	4248	9.8
Chita (this paper)	*c*. 2000	30° 28.8'S	69° 39.5'W	4150	4638	4038	600	1515	555	21.6

Alt.pf: Altitude permafrost estimated from Gruber's (2012) model; Alt. max: maximum altitude of failure; Alt.min: minimum altitude of landslide deposit; H: altitude difference; L: horizontal length of landslide development; La: excessive travel distance (cf. Hungr, 1990); Fb: fahrböschung (angle formed by the landslide's vertical and horizontal travel distances); ??: unknown date of the landslide.

Permafrost and Landslide Occurrence

Permafrost aggradation or degradation, as defined solely on the basis of temperature, takes place due to complex interactions between the surface-atmosphere energy exchange, seasonally variable ground surface and sub-surface thermal characteristics and geothermal heat flow (Washburn, 1973; Lachenbruch *et al*., 1982; Duguay, *et al.,* 2005). However, the ice content in the ground, besides altering soil thermal conduction due to ice to water phase change that is highly energy-consuming, is the key factor for dramatically changing some physical characteristics. Soil ice content is the parameter detected by indirect geophysical surveys and one of the main concerns in engineering procedures as it strongly influences soil strength and slope stability. Ice acts as cement in loose, immature granular soils on arid-region gravelly slopes formed by rock-fall, colluvial and/or alluvial processes, where in the absence of vegetation, there is little clay and organic matter.

The relationship between landslide activity and the degradation of ice-rich permafrost should be straightforward: if a steep slope is kept stable by ice cement, melting of the ice will create soil instability that could lead to a catastrophic collapse. In utilising this concept, this paper will try to demonstrate how molards may help to identify permafrost-related landslides and elucidate the trigger of these failures, including those that end in fjords.

There is consensus that many processes of global change will increasingly cause natural hazards (Intergovernmental Panel on Climate Change, 2007; Clague *et al*., 2012; Zischg *et al.*, 2012), but how this occurs is still a matter under study. Among these hazards, landslides have caused thousands of victims. Permafrost degradation may lead to an increased number of natural hazards; climatically driven degradation of rock-wall permafrost is a recognised trigger of rock-falls (Deline and Ravanel, 2011; Kellerer-Pirklbauer *et al*., 2011). Zischg *et al.* (2012) also indicated that the most important consequences of permafrost degradation to infrastructure are slope movements and rock-fall processes. Therefore, any new indicator of permafrost degradation might be useful for detecting and monitoring possible risk areas due to permafrost-bearing landslides.

Regional Permafrost Degradation Indications

Permafrost degradation in the arid mountain region of the Andes extending from *c*. 31° to 23°S seems to be dominated by the loss of soil ice content through precipitation deficit rather than atmospheric warming. This region is currently water limited, and so during winters the active layer does not recover the complete ice content that it can hold (Croce and Milana, 2002). During droughts, the ice formed in winter in the active layer is limited or absent, allowing the summer thermal wave to penetrate deeper in the ground than it would in more ice-rich conditions since there is less energy employed in melting the seasonal ice. Thus, progressive loss of ice from the top of the permafrost could occur in this situation. Though only anecdotal evidence exists for a water deficit-driven ground ice loss in the arid Andes, there is good evidence to suggest a sustained reduction in snow precipitation at this latitude in the Andes (Rutllant and Fuenzalida, 1991; Minetti and Vargas, 1998; Rivera *et al.*, 2000; Luckman and Villalba, 2001; Minetti *et al.*, 2003; Intergovernmental Panel on Climate Change, 2007; Vuille and Milana, 2007). Studies comparing the only long record of snow precipitation in the area (the Indio Mine) and rainfall at two cities near the Pacific coast showed a strong correlation (Vuille and Milana, 2007), which suggests that the city of La Serena, with a long precipitation record, provides a proxy of snowfall in the high Andes Cordillera. Using this reasoning, it is suggested that snow precipitation decreased to half over the last recorded 130 years, while air temperatures did not change significantly. It is therefore inferred that the permafrost soils of the arid Andes have been drying out and losing ice during the last century. The effect of this may be a reduction in soil strength as the cementing role of

the ice matrix diminishes, making the slopes more prone to mass movement.

Hypotheses of Molard Formation

Brideau *et al.* (2010) reviewed five different hypotheses for molards and proposed a sixth. The first hypothesis took into account the fact that debris at the sides of molards was finer grained than the surrounding landslide debris. Thus, Goguel and Pachoud (1972) suggested that the finer debris accumulated around large boulder cores when the landslide was slowing down until coming to rest.

The second hypothesis, proposed by Cassie *et al.* (1988), suggested that the cones resulted from ground vibration produced during landslide movement. These authors supported their interpretation since small cones of loose material (sand from 0.05 to 2 mm) were formed under laboratory conditions when the material was placed over a vibrating table, and some grain size segregation resulted between the cones and the rest of the material. The sequence of artificial cone formation is summarised as follows (after Cassie *et al.*, 1988). (1) Segregation of the coarser grains, which rise to the top of the deposit immediately after vibration begins. (2) Cone build-up, with coarser particles emerging from the cone tops. (3) Shoulders of the cones become depleted of coarse particles, whereas fine particles exhibit a cyclic motion of entering the cone, moving to the top and sliding down the sides. (4) When all of the coarse particles have been expelled, the mounds lose their peaks and became more rounded. Thus, the experiment generated rounded mounds of exclusively fine material, while the spiky ones had a chimney of coarser material surrounded by finer-grained material around the sides of the cone.

The third hypothesis (Dufresne and Davies, 2009) was not specifically elaborated for molards, but rather for hummocks on landslide deposits. The hummocks, perhaps the result of molard degradation, were attributed to the formation of linear ridges that are the result of grain size segregation and flow front perturbations. If the flow expands, ridges tend to evolve into hummocks. However, most examples described are rounded and not conical, except for a few cones mentioned for the Jocotitlán debris avalanche deposit (Siebe *et al.*, 1992) that are one or two orders of magnitude larger than maximum sizes reported for molards (*c.* 5 m high).

A fourth hypothesis was proposed by Shreve (1966) after his study of the Sherman glacier landslide which he suggested was emplaced by moving over an air sheet trapped below the debris mantle. Thus, molards were formed by the release of excess pore pressure of fluids trapped by the slide. Evans *et al.* (2009) modified this hypothesis by proposing that the fluid escaping was water, similar to the process that produces sand volcanoes in other sedimentary environments where sand becomes fluidised and over-pressured (Reineck and Singh, 1979).

A fifth hypothesis is that molards develop by a secondary cohesion generated by friction between two layers moving at different velocities along transport-parallel strike-slip faults (Shea and Van Wyk de Vries, 2008). However, the hypothesis applies for larger-scale hummocks, such as those considered by Dufresne and Davies (2009), and was not intended to apply to molards.

The most recent (sixth) hypothesis, proposed by Brideau *et al.* (2010), attributes molards to the degradation of ice-cemented boulders formed by granular material. This hypothesis resulted from the discovery of ice-cementing open-framework gravels in some proto-molard blocks.

Hypotheses 3 and 5 relate to the generation of the hummocky relief of some mass-wasting deposits, and do not necessarily comply with molard description. A distinction should be made between hummocks and molards. Molards are almost perfect steep-sided cones, show a clear grain size gradation at the surface and have a rather particular internal structure (as depicted by Cassie *et al.*, 1988, and shown hereafter), whereas these three elements would not be observed altogether on hummocks. Old, degraded hummocks may also exhibit a skirt of secondary material produced by slope degradation. Thus, one of the objectives of this contribution is to better characterise molards in order to clarify their distinction from other forms produced over a landslide.

Molard Occurrence

Molards have been mentioned on the Khait slide (Evans *et al.*, 2009), the Yigong rock and debris avalanche (Qiang *et al.*, 2012) and the Sale Mountain landslide (Zhang *et al.*, 2002) in Asia, while in North America they have been reported in the Frank slide (McConnell and Brock, 1904; Cassie *et al.*, 1988), the Sherman slide, just as 'cones' (Marangunic and Bull, 1968) and 'xenolithologic debris cones' (Shreve, 1968, page 400), the Little Salmon Lake landslide (Brideau *et al.*, 2010) and the Pink Mountain slide (Geertsema *et al.*, 2006) (Table 1). Undocumented molards are probably present in many other landslide deposits.

On account of the permanent and progressive transformation of molards since the emplacement of the debris avalanche, only relatively fresh debris avalanches may help in understanding the origin of molards (cf. Brideau *et al.*, 2010). In the present paper, an opportunity to study molard formation was provided from a relatively recent debris avalanche, which was sourced from a body of permafrost and produced numerous molards. Additionally, the importance of this example to understand these cones also relies on the presence of molards detached from the body of the debris avalanche deposit.

METHODS

This study tests the hypothesis that molards can be produced from the thawing of fragmented and rounded intact blocks of frozen landslide debris, although not necessarily in all cases (as expected for cones in the Sale Mountain slide). Four approaches are used to test this hypothesis: (1) a review of

the known global distribution of molard-bearing mass movements with respect to permafrost distribution (Table 1); (2) a field survey of a recent landslide (the Chita landslide in the Andes of Argentina) that unequivocally relates to permafrost failure, as discussed in this section; (3) a detailed survey of the external and internal structure of molards, applying for the first time micro-sedimentary transport concepts to molards; and (4) the generation of artificial molards by laboratory simulation using frozen ground.

The literature review of molards and debris cones found that molards are not always explicitly described, as in the case of the Sherman and Seit slides. After recognition of the traditional shape in the published pictures, morphometric data were obtained from the published literature and controlled using the available existing systems for global imagery (e.g. Google, Bing, Yahoo). In some cases, morphometric data were corroborated using the elevation models of these systems.

A field survey of the Chita landslide was carried out during April 2012, associated with new mining works in the Chita valley. Depositional angles of the deposit and features such as lobes and superimposed cones (see Figure 2) were measured, and landforms were mapped using satellite imagery. Satellite imagery used was basically high-definition images of Google Earth and Bing, but determination of the time of occurrence was made with the Landsat archive of the United States Geological Survey as the landslide predates timing of the publication of high-definition satellite images. To obtain a high-resolution caption of the basin before the landslide (see Figure 1), an aerial photograph was searched in the SEGEMAR (Servicio Geológico y Minero Argentino) photo archive. Many molards were excavated to inspect their internal structure, although the best example of this was provided by a molard cut naturally by the Chita Creek. The description of the internal structure was combined with the description of the granulometry of the

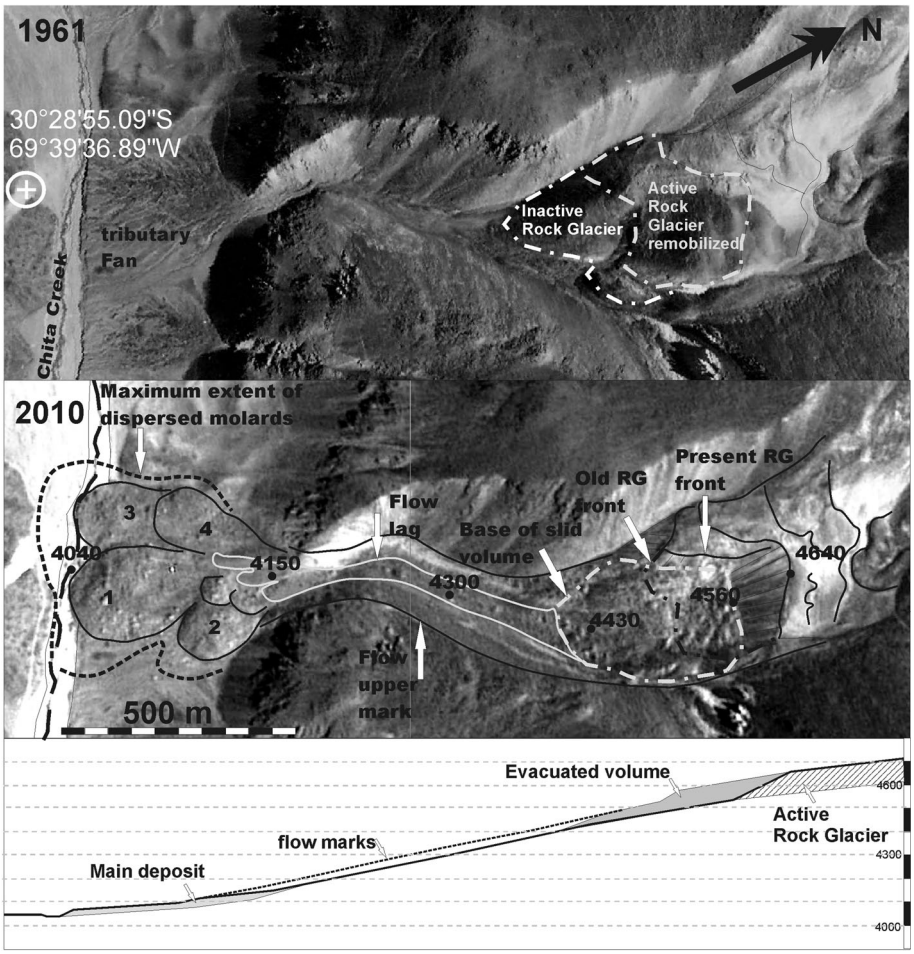

Figure 1 Chita Landslide. Upper: View of the tributary valley in 1961 (coordinates marked), showing an active rock glacier and a lower inactive lobe. Middle: Present shape of the same valley as in a 2010 image. Black circles mark heights (0°C isotherm is at *c*. 4200 m), and rock avalanche lobes are numbered according to the expected formation order. Lower: Schematic topographic cross-section of the source area and rock avalanche deposit. The geometry of this debris avalanche is given by: height = 600 m (from 4638 m to 4038 m asl), length = 1515 m, excessive travel distance = 555 m (1515 m - 960 m) and fahrböschung (angle formed by the landslide's vertical and horizontal travel distances) = 21.6°. RG = Rock glacier.

external deposit and the sedimentary facies identified within the molards. Traditional sedimentary analyses were used to describe the sediments and interpret the origin of the different meso-units recorded in the molards.

Laboratory simulation of molard formation by analogue modelling was performed using a laboratory freezer in Marburg University to create artificial permafrost blocks (Marburg/Lahn, Hessen, Germany). Three different types of sediment aggregates were frozen into isometric blocks (spheres) using moulds that allowed complete water saturation of the sediment. Sediments used were; (a) fine sand; (b) fine, medium and coarse sand; and (c) granule-rich medium to coarse sand. Once perfectly frozen (one sphere was broken for testing), the spheres were left to thaw at ambient room temperature (*c*. 20 °C). Two different sizes of spheres were tested: a first and second set using (a) and (b) sediments of *c*. 7 cm in diameter in which blocks were carved out of bigger blocks, and a third set of *c*. 14 cm in diameter using spherical bags as moulds using (c) sediments. Once frozen, simulated permafrost blocks were left over plates at room temperature including a few hours per day under direct exposure to sunlight, and their evolution recorded every *c*. 12 h, for a complete run of 1 week.

THE CHITA LANDSLIDE AND ITS MOLARDS

Study Site

The study site lies within the central arid Andes, which is characterised by a winter snow regime mainly produced by easterly winds carrying moisture from the Pacific Ocean. Snow precipitation events relate to polar fronts expanding northward but flowing eastward. As a result of the north-south axis of the main Cordillera, precipitation is usually forced at the highest part of the Cordillera, while dry and warm air descends as a katabatic wind called Zonda. The Andes Cordillera is high near the study site, with passes not below 4800 m asl and maximum summits at 6300 m asl. On account of the marginal effect of polar fronts at this latitude, snowfall is low and as a result of aridity, the lower limit of uncovered glaciers is between 5000 and 4700 m asl and the theoretical snowline is located higher than many of these glaciers (Kull *et al.*, 2002). While uncovered glaciers are scarce, rock glaciers are widespread, indicating that ground ice survives better in this climate regime than exposed glacier ice.

The Chita landslide occurred in 1996 according to imagery available for the site. The landslide debris travelled the length of its source tributary, spread out onto an alluvial fan adjoining the Chita River valley and crossed the Chita River, producing a total run-out distance of 1.5 km (Figure 1). This deposit is well suited to understanding the origin of molards due to: (a) recent formation, thus the natural degradation of the elements is limited; (b) the protolith or source material feeding the flow is confidently established as an active rock glacier terminus, as explained in the next section; (c) the flow produced several lobes, indicating that it moved as a sustained debris avalanche, not as a coherent slide; (d) most of the terminal flow deposit is blanketed by molards; (e) a large molard was recently cut by river erosion, allowing a detailed study of its internal structure; and (f) there are many 'outrunners' (boulders detached from the main avalanche lobe, *sensu* Nissen *et al.*, 1999; De Blasio *et al.*, 2006).

The Failure

The failure at the source area was occupied by a rock glacier (Figure 1), which based on its morphology appears to be partially active. Active rock glacier activity at this elevation (4450 to 4650 m asl) is consistent with the thermal conditions expected there (0 °C isotherm is at about 4200 m asl; Milana, 2006) and the presence of active ice-bearing permafrost features such as rock glaciers and protalus lobes being observed at elevations as low as 4150 m asl in this area (Schrott, 1991; Croce and Milana, 2002; Milana and Guell, 2008). In this region, the global permafrost model of Gruber (2012) also estimates favourable permafrost conditions starting between 4000 and 4200 m asl. The geomorphology of the failed rock glacier terminus and the small, low-altitude cirque lacking clear evidence of a pre-existing glacier suggest that the rock glacier developed a sediment-rich permafrost core from the accretion of colluvial beds and snow-rock debris avalanches (i.e. cryogenic rock glacier) rather than by burial of a glacier (i.e. glaciogenic rock glacier; see Croce, 2006; Milana and Guell, 2008; Milana, 2011). However, this interpretation is preliminary as Croce (2006) demonstrated using electrical tomography and seismic refraction that some presumed cryogenic rock glaciers are glaciogenic due to the large massive ice cores imaged. In the absence of detailed studies, the author interpreted that this particular rock was formed by the piling up of sediment and snow, therefore the ice content in the permafrost core would be relatively low.

In 1996, an area of approximately 7 ha detached from the rock glacier front and travelled down the valley. Given the *c*. 80 m high rock glacier front, an estimated volume of $5.6 \times 10^6\,m^3$ flowed down to the main valley in this event. Part of the rock glacier front was only locally displaced along normal faults as a block on the west side (Figure 1), while some blocks which were left near the slide scar subsequently thawed and became molards. The material was sourced from 4450 to 4650 m asl and the landslide main deposit lies between 4050 and 4150 m asl, and so most material crossed the local 0 °C annual isotherm that is at *c*. 4200 m asl. Because the valley faces south and the rock glacier was active, most of the slid volume probably comprised permafrost. The presence of nearby cryogenic rock glaciers at comparable altitudes suggests that the top of ice-cemented permafrost could be located as deep as 5 m (Croce and Milana, 2002; Milana and Guell, 2008), while the upper part could be cryotic but unfrozen due to the lack of water in this arid environment. It is thus estimated that *c*. 80 per cent of the volume was ice-cemented permafrost. Because the temperature has been

fairly stable over the last decades, the failure may have developed as a result of a loss of cementing ice due to the long drought from 1993 until 1996, while possible triggering would be caused by the effect of overloading the slope by the winter snowfall.

The Flow

The initial collapse was probably a rotational failure that generated an initially coherent landslide, as suggested by the concave slide scar. There are several slide blocks near the scar and some tensile fractures parallel to the scar within the remaining rock glacier front. Flow progression would produce block fragmentation, reshaping the blocks of frozen ground into isometric aggregate boulders with the flow developing into a debris avalanche. The rapid block fragmentation is indicated by the presence of a boulder lag distributed along the bottom and perched on both sides of the tributary valley. Lubrication of the flow by snow is inferred because: (1) almost no free mud was found between blocks, and only a small amount of mud was a component of the internal structure; (2) rain is rare and meltwater is usually scarce and drains rapidly in this environment; (3) a lubricant is needed to explain the excessive travel distance; and (4) the occurrence of outrunners on top of the opposite river bank suggests that a thick mantling of snow in the Chita Creek would have lessened any barrier created by the opposite terrace step. This would help to explain the position of the isolated 'boulders' that rolled outwards from the avalanche lobes that then evolve into molards (outrunners). This last evidence is the strongest as the opposite river bank commonly forms a step significantly larger than the expected original diameter of the outrunner block (see Figure 2A).

The initial flow seems to have had an advancing head of higher viscosity. This is interpreted from the good match

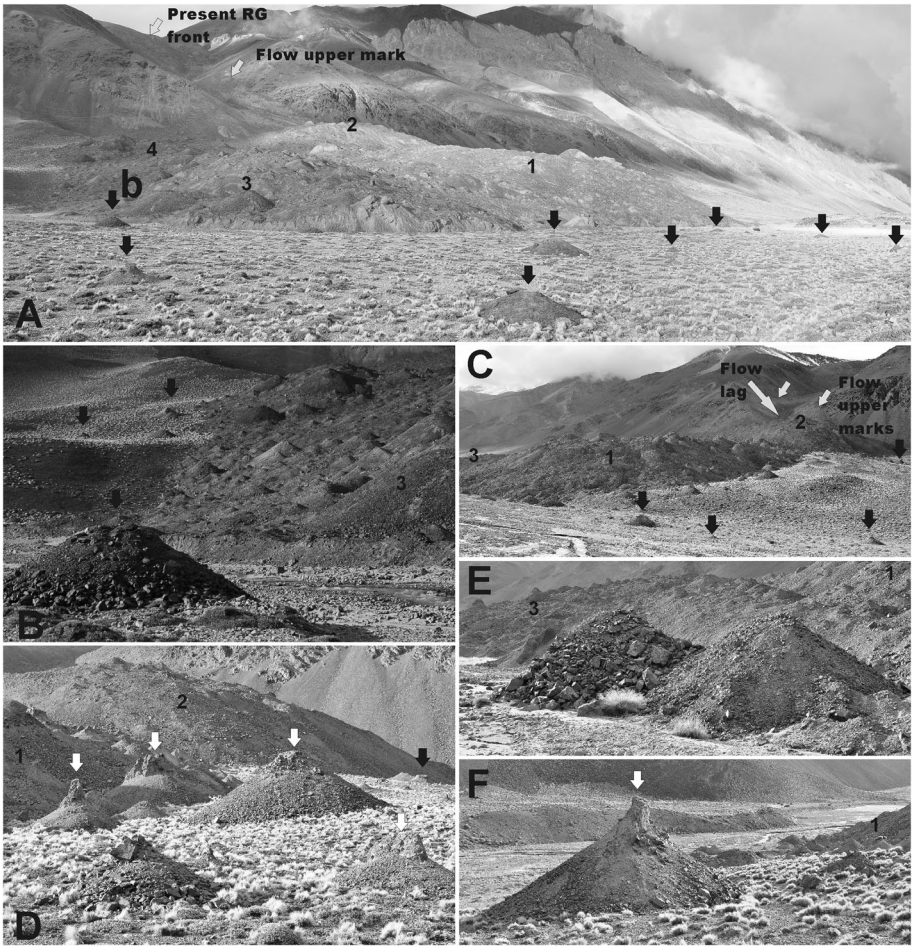

Figure 2 Chita Landslide. The rock avalanche and external shape of molards. (A) View from southwest of the avalanche with numbered lobes (Figure 1), black arrows indicate conical molards detached from lobes, white arrows in C and F, are molards with the boulder core still protruding over the microtalus and b is the molard in (B) that shows less microtalus slope and good colluvial (gravitational) downslope sorting. Note the molards spread out across the terrace, with the Chita River channel between the photographer and the slide deposit. (C) View from southeast of the avalanche, detached molards and flow pathway in the tributary valley. (D–F) Molards at different stages of evolution from an original protruding boulder core with vertical slopes (F) to most conical and finally rounded shapes (D, E), also showing large compositional differences (E) explaining the 'xenolithological' cones of Shreve (1966) as a result of boulder mixing during the flow. RG = Rock glacier.

between the highest flow marks along the conduit valley sides, defined by a thin sheet of debris material with stranded boulders and molards on both valley sides, and the topographic top of depositional lobes 1 and 2 (Figure 1 lower and Figure 2). The viscous head would have retained part of the flow upstream that would evacuate the conduit subsequently and form lobes 3 and 4. These lobes formed later and are flatter and continuous with the lower marks along the tributary valley, suggesting that the flow became more fluid over time, allowing part of the material stranded on the valley to be re-entrained in the flow at its latter stages. The flow was incoherent, since it was possible for boulders to move ahead of the lobes observed as 'outrunners' associated with all main depositional lobes. This behaviour is comparable to high-slope mud-lubricated blocky debris flows (video 1 in the online Supporting Information) but in this case, snow was probably the main lubricant due to the absence of mud films or a 'splash' (cf. Hungr, 1990). The progressive flatter and longer lobes, suggestive of an increasingly lubricated (and/or more dispersed) flow, may record entrainment of snow (and possibly frictional melting of that snow) during transport.

Main Deposit

Approximately 90 per cent of the landslide debris was deposited on the alluvial fan abutting Chita Creek (Figure 1), covering *c*. 11.5 ha of the tributary alluvial fan and the Chita River stream bed. The debris avalanche produced four main lobes, partly superimposed, numbered as they formed. The maximum thickness of individual lobes is estimated to be 20–30 m. Frontal and lateral slopes of lobes 1 and 2 are commonly 30–40°, sometimes reaching up to 45°, although this is a secondary slope formed after boulder degradation. Lobes 3 and 4 have marginal slopes between 22 and 27°. The projection of the topographic surface of lobe 2 (Figure 1) coincides with the upper mark of the flow on the eastern valley side, suggesting that it formed when the flow viscosity was at its maximum. After deposition of lobe 2, the flow started to erode and rework part of its deposits into lobes 3 and 4, which show much less relief and therefore indicate a less viscous flow. All four lobes are covered by molards.

Molards at the Chita Slide

As about 80 per cent of the flow was made up of ice-cemented permafrost, most avalanche boulders would have lost that ice because they were transported below the expected location of the 0 °C isotherm near 4200 m asl. Thus, boulders were reshaped into molards, probably within months to a couple of years, that today blanket depositional lobes and parts of the tributary valley side and bottom. Most molards directly overlie the debris avalanche deposit, with an abnormally high density compared to any other molard-bearing deposit. However, a few molards, identical to those over the main deposit, formed as isolated cones directly over the pre-existing alluvial tributary fan and over the Chita Creek stream deposits, as discussed below.

Morphology.

Chita molards are estimated to be (at the time of the survey) 16 years old according to the available imagery. Today, they show several shapes, possibly due to differences in the original boulder shape, composition and internal cohesion after ice melt-out, giving place to differential degradation rates. The possible original shape of the boulders was investigated on isolated molards detached from the avalanche body, since the boulder volume could be estimated from the final molard shape. Differential degradation has resulted in some molards having part of the original debris boulder still intact and protruding above partly degraded molards in the form of *c*. 45° cones (Figures 2F, Figures 5 and Figures 6). The debris boulder in such molards appears to remain intact due to weak (friable) cohesive cement. Such weak cohesion observed is unlikely to have played a significant role in keeping the boulder in one piece during avalanche motion (without the additional forces of ice). For most molards observed, the original boulder has been completely reshaped into a cone (Figure 2E). Some cones are almost perfect, sloping between 45 and 35° (Figure 3), while others are flatter with maximum slopes of 30° and rounded tops. At a nearby molard-bearing avalanche of *c*. $>$ 25 years old (Figure 4B), all detached molards were much flatter (slopes $<$ 30°) and none had traces of the original boulder outstanding at the centre, suggesting that cones progressively degrade over time, resulting in gentler slopes and rounder tops. Each molard excavated at Chita Creek revealed the original conglomerate to breccia boulder coring it, below an irregular skirt of better-sorted and usually finer-grained colluvial sediment (microtalus). Differences in degradation are likely the result of differential cohesion of boulders caused by the original depositional processes forming the colluvial breccia/conglomerate before it became ice cemented during rock glacier formation. Microclimatic factors such as sun or wind exposure and grain size distribution (as more clays enhance cohesion in this material) may also play a role. Differences in cone slope and shape can be related to the original boulder shape (see the Discussion).

Outrunners.

Many molards on the Chita slide were completely detached from the main deposit (Figure 1 marks their maximum extent). The more distant isolated molards were surveyed at distances of *c*. 100 m from the main deposit edge and occur today on alluvial surfaces. Isolated molards are interpreted to result from the degradation of outrunners. Outrunner blocks are nearly intact masses of debris detached from a retarding mass flow that travels beyond the flow front (Nissen *et al.*, 1999; De Blasio *et al.*, 2006) and are mainly observed in submarine landslides. Descriptions of outrunner blocks are rare, and their intrinsic scarcity is perhaps the result of detection problems since they are relatively tiny seabed features. Submarine outrunners usually glide away from the flow front but they may roll as well (De Blasio *et al.*, 2006).

Molards produced from outrunner blocks today are burying plants as the original boulder slowly degrades. Their position over pre-existing terraces indicates that: (a)

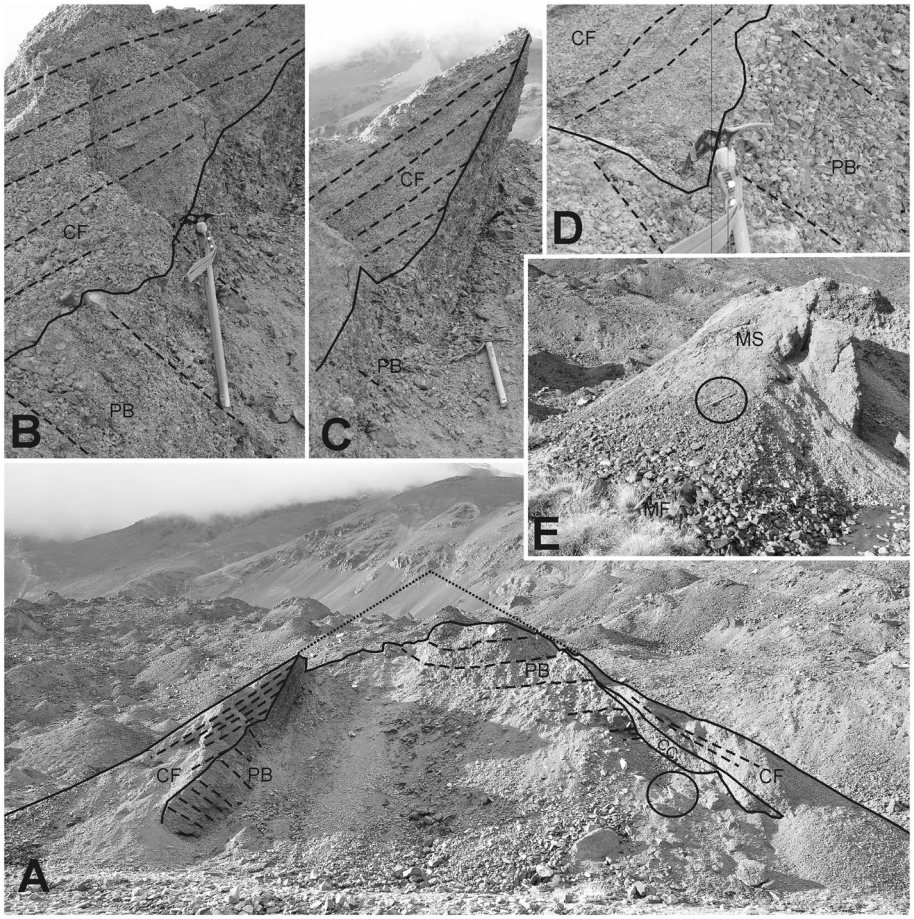

Figure 3 Internal structure of molards. (A) Cross-section of a 5 m tall, 15 m wide molard, eroded by the creek. The permafrost boulder (PB) is easily distinguished from colluvial flows (CF) and colluvial collapsed (CC) sediments. (A–C) Details of the permafrost boulder composition are interpreted locally as rhythmic colluvial sediments, quite comparable to the recent colluvial flow sediments. Note the coarser colluvial flow sediments downslope in (B), and the open framework of the sediments forming this part of the boulder. (B, D) Ice axe encircled is 58 cm long. (E) Gravitational sorting along the microtalus of the eroded molard leaving finer grained sediment over microtalus slope (MS) than in floor (MF). PB = Permafrost boulder; CF = colluvial flow sediments; CC = colluvial collapsed sediments; MS = microtalus slope; MF = microtalus floor.

outrunners were capable of rolling or sliding over the ground without breaking until they came to rest; and (b) there was probably a snow blanket smoothing the topography in order to allow outrunners to roll over the opposite terrace step (Figure 2). The maximum distance of outrunners from the main deposit edge is always in the orientation of the local terrain slope. The size of the isolated distal molards is variable, but their distribution shows a rough size sorting, with smaller molards having travelled farther than the larger molards. This sorting may have been produced by an excess of basal friction in respect to the effect of direct gravitational force, since the opposite happens in a colluvial system in which larger components advance further than smaller ones (see below).

Boulder Source.

Exposures of the intact landslide boulders in excavations and natural cuts provided sections to study the original depositional processes that formed the sedimentary units of the slide, before becoming ice-cemented permafrost. The units consisted of sandy conglomerates to breccias with different textures and structures. They can be grouped into two main sedimentary classes: (a) massive and poorly sorted breccias, clast to sand matrix supported, sub-angular, suggesting that they were deposited by mud-poor debris flows; and (b) well-stratified, sometimes rhythmical, clast-supported, sub-rounded to sub-angular and moderately sorted mud-free gravel that is comparable to sediments of local talus. This rhythmic type of stratification has been observed in colluvium as a result of debris fall (Blikra and Nemec, 1998) that produces open-framework angular gravels, fining upwards. During intervals of no transport, local intense winds would cause the surface to accumulate wind-borne matrix, and some water flows might also add fine matrix to these layers, creating this rhythm. The sedimentology observed in the interior of the boulders suggests a cryogenic origin of the failed rock glacier terminus, as explained above. These mud-free to mud-poor gravel

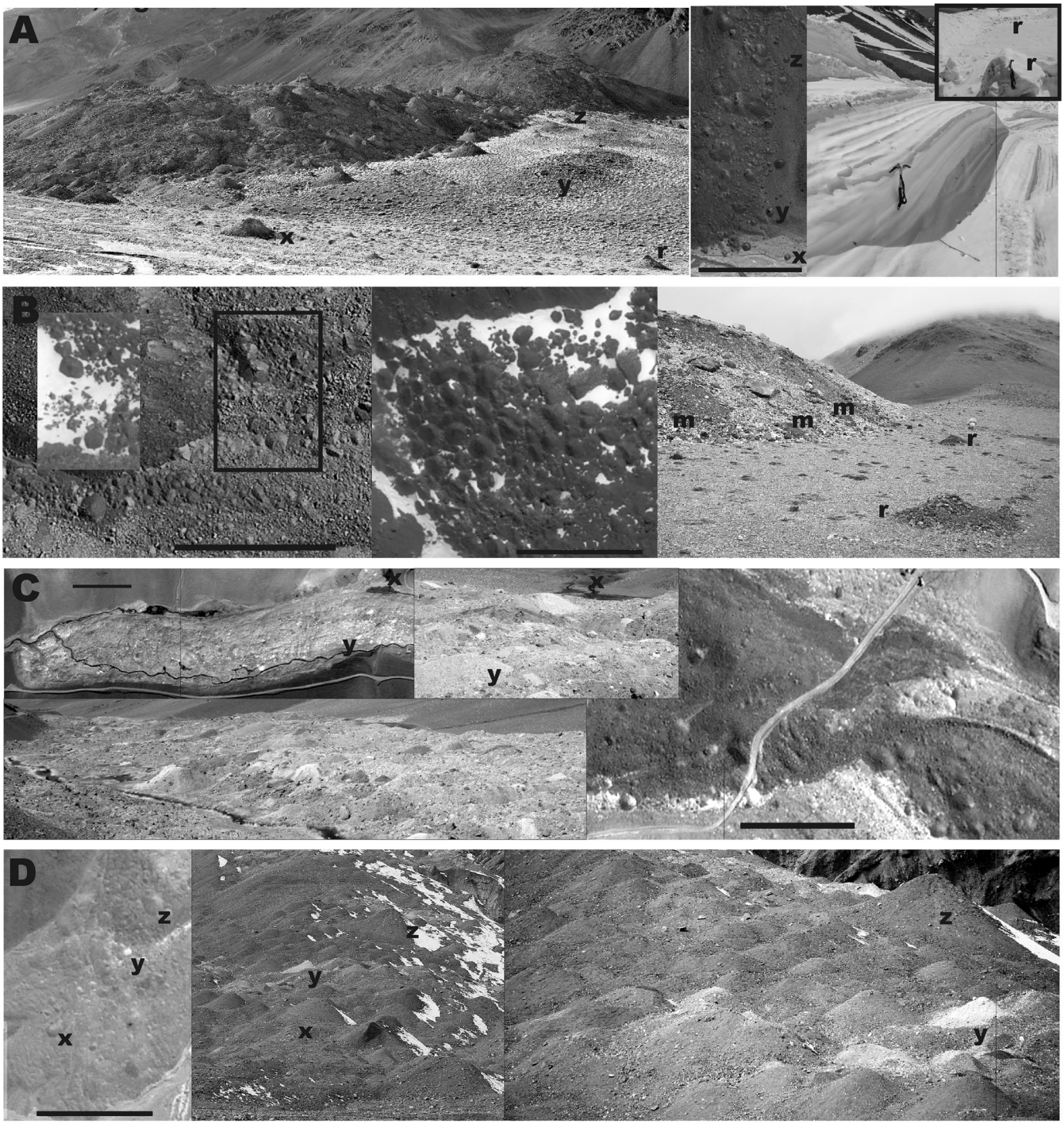

Figure 4 Four examples of molards observed in different landslides in the field that could also be recognised on images. (A) The Chita slide (30°28'46.40"S, 69°39'31.22"W), with outrunners sideways from the flow as shown on image, and a comparison to a snow slab avalanche (extreme right of Fig. 4A) also showing slide planes as observed in the Pink Mountain slide (Geertsema *et al.,* 2006). (B) The San Lorenzo slide (30°15'26.50"S, 69°49'44.96"W) that evolved into a rock glacier, showing a few outrunners. Inset of left image of Fig. 4B, shows rectangled area in winter with fresh snow, that allows marking the circular base of the molards. (C) The Altares West slide (31°30'32.97"S, 70°32'4.20"W) also showing molards and the effect of damming tributaries. The fahrböschung of 9.8° is extremely low. (D) The Erizos South slide (31°42'24.41"S, 70°16'37.54"W), a much older slide but still showing molards. Note the different composition of molards marked x, y and z. Bars on images are 100 m; x, y, z are homologous points on image and field photographs; r marks outrunners; m, molards.

boulders (Figure 2) would not survive the 1.5 km of avalanche transport without breaking down into their clastic components. Their survival during transport can only be explained by ice cementation, supporting the hypothesis that they were ice-cemented permafrost boulders. When these boulders were emplaced at the fan, below the 0 °C isotherm, all ice-cored permafrost would have begun thawing. Ice from the upper 5 m of sediment probably melted during the first summer, based on the penetration depth of seasonal thermal waves in the region at comparable altitudes (Trombotto and Borzotta, 2009), and perhaps some ice still survived a few years longer within the lobe cores.

Internal Structure.

A molard 5 m high and 12 m wide, cut by the Chita Creek, showed a well-defined contact between the original boulder and the debris skirt formed during boulder degradation (Figure 3). The boulder coring the molard was stratified. One part of the section was composed of a non-stratified and unsorted sandy-silty matrix breccia (right, Figure 3A), passing into a well-bedded and sorted gravel, stratified in alternating couplets of open-framework and matrix-rich clast-supported gravels (left, Figure 3A), suggesting that this particular boulder was formed in a colluvial environment where normal debris fall deposits were intercalated with mass transport deposits. At this molard, a clear boundary between the original permafrost boulder and the microtalus draping was observed (Figure 3).

Microtalus.

As colluvium is mainly transported as a result of gravity and not by fluid shear stress like alluvium, momentum gained by fragments depends on their mass and facility to roll. Thus, bigger clasts move farther downslope, causing colluvial talus to show downslope clast coarsening, as opposed to downstream fining of alluvial fans (Blikra and Nemec, 1998). In molards, the bigger stones released off the permafrost boulder were capable of rolling to the cone base and even beyond, sometimes outrunning the base by a few centimetres. The smaller stones were arrested at higher, intermediate positions, while the finest grains remained mostly near the top. Because the large stones mix and camouflage with the ground (usually the upper surface of the avalanche deposit), the finer-grained part of the microtalus is usually more visible and evident. This simple process explains the well-observed and elusive grain size difference between molard core and draping microtalus, identified by different authors as bimodality (Cassie *et al.,* 1988) or xenolithologic (Shreve, 1966). The early process would involve the direct gravitational fall of stones over boulder irregularities and no clear stratification was observed in the cuts (Figure 3), whereas after a continuous slope is formed, typical colluvial transport produces a layered deposit. The same rhythmic stratification of colluvium was also observed in cuts of the microtalus, suggesting that transport was as debris fall. Microtalus dynamics thus explain the overall observed bimodality of molards (Cassie *et al.*, 1988) and the sediments draping molards being finer grained than the core itself. Therefore, dating of the lower beds of microtalus could indicate the minimum age of the molard-bearing landslide.

LABORATORY SIMULATION OF MOLARDS

A simple simulation of molard formation by degradation of an ice-cemented conglomerate was carried out under controlled laboratory conditions. This simulation differs significantly from the experiments of Cassie *et al.* (1988), where cones were generated by a vibrating table, testing the hypothesis that cones were formed by the vibration produced during the avalanche. Three sets of different sediment aggregates were tested, as discussed previously. The first set (made of fine sand) failed to produce good conical molards due to the natural internal cohesion with minimal moisture content, and the low repose angle, once dry. The internal cohesion tended to keep the boulder together until it broke apart completely,

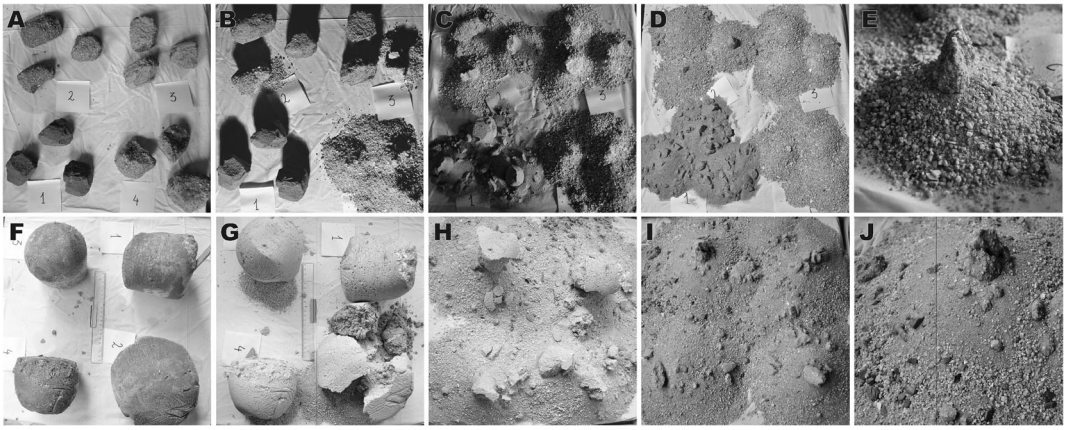

Figure 5 Laboratory simulation of molards. (A–D) Evolution of permafrost blocks ~ 8 cm in diameter of different composition, taken at about 6 h intervals: paper labels in each caption correspond to, 1: fine sand; 2: fine; medium and coarse sand; 3–4: granule-rich medium to coarse sand. (E) Detail of a molard labeled as 2, in Fig. 5 A to D, after 24 h. (F–I) Evolution of larger (16–20 cm large) permafrost blocks made of gravelly sand, taken at *c*. 2 day intervals. (J) Detail of (I), showing grain size segregation along the microtalus, leaving finer-grained sediment over the upper cone skirt.

producing smaller blocks. The second set (coarse sand with different proportions of fine sand and fine gravel) created well-defined cones. However, owing to the small size of the simulated boulders, colluvial transport (e.g. the gravitational movement of grains once released from the thawing block) was limited to just 2 cm at most and thus vertical grain size segregation seen in real molards was not observed. The largest blocks of the third set (assorted fine and coarse sand with granules) degraded well into cones and also showed good sediment grain size segregation in a 10 cm long micro-talus. In successfully simulated cases, blocks initially passed through a stage where the original block was protruding and flanked by a conical micro-talus (Figure 5), until they degraded further into a flat cone due to the low natural angle of repose of the sediment used, differing from the debris observed on most real molards.

Another interesting finding of this experiment is the remarkable analogy with the 'cellular' morphology observed on satellite imagery showing a dense occurrence of molards and the plan shape when laboratory boulder degradation was complete (Figure 5D and Figure 5I). This 'cellular' morphology would be produced by the coalescence of cones and would be only the case of a surface originally made almost exclusively out of permafrost blocks that evolved into cones. This term is introduced here due to the resemblance of this pattern to the irregular boundaries formed by some organic cells in section. This morphology has been observed by the author in old sub-aerial and sub-aqueous avalanches expected to be formed of permafrost, present in Norwegian fjord environments (e.g. 68°56'28.58"N, 15°1'3.65"E). Four examples of this morphology are shown in Figure 4. This cellular-like plan view of moderately degraded molards may help in recognising and interpreting the origin of many recent landslides in periglacial regions.

DISCUSSION

Geometrical Considerations of Molards

Assuming a clast-supported and ice-cemented boulder that becomes isometric due to fragmentation and abrasion during transport, the projection of vertically released fragments on the ground is not a cone, but rather a shape with steep sides and a rounded top. However, if it evolves into a cone of the same height (height equals the diameter of the sphere), the angle of the side would be 51.9° (and the cone radius would be πd/2). The maximum angle of repose of loose debris or rubble is *c*. 45° in field surveys and field conditions (cf. Kleinhans *et al.*, 2011; Jun-Jie *et al.*, 2013), coinciding with maximum slopes measured at the Chita slide cones. Thus, the resulting geo-form after ice melting will rapidly be a 45° sloping cone (Figure 6). If there is some cohesion, and given the fact that for the same volume, the diameter of a sphere is larger than the height of a cone with 45° slopes, some parts of the original block will protrude at the cone centre for some time, until the exposed top of the boulder core degrades into the micro-talus. Alternatively, if an impact broke the isometric boulder into two halves, a semi-sphere would degrade into a cone of only 32.5° average slope (cone height would equal the radius of the half sphere, r, and cone radius would be πr/4). Given that the initial angle of repose of the composing debris is 45°, a boulder of this shape (plus other types as slabs or less isometric shapes) will also degrade into a micro-talus but create a rounded-top cone having almost the same original height as the boulder. The micro-talus will likely be formed from the mid-height of the cone to the base.

Therefore, molard shape depends largely on the shape of the precursor boulder, explaining the wide range of cone slopes and shapes observed in deposits having the same age and composition (e.g. Brideau *et al.*, 2010). As Chita molards were produced by permafrost in a cryogenic rock glacier, most boulders were ice cemented, creating almost perfect cones in most cases. However, other permafrost failures could involve a larger variety of precursor material, including boulders made of massive ice, or having patches of pure ice owing to the fact that many local rock glaciers show pure ice cores (Croce and Milana, 2002; Gestión Ambiental Consultores (GAC), 2012), creating irregular, not necessarily conical, molards.

Isolated Molards and Outrunners

The appearance of distal isolated molards, detached from the main lobe, has been observed in other debris/rock avalanches in the region (Figure 4). The possibility of debris rolling beyond the main deposit has been observed in many snow slab-block avalanches, which may also show sliding

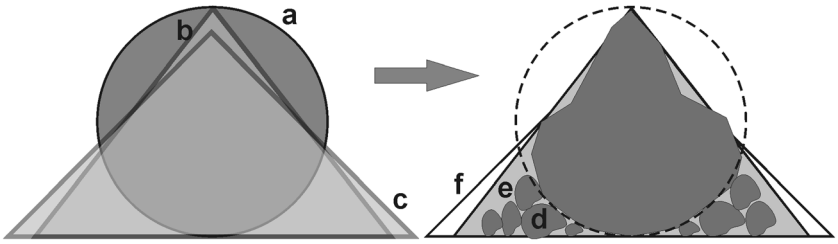

Figure 6 Theoretical and schematic evolution of an isometric ice-cemented conglomeratic boulder whilst thawing. On the left, the initial sphere (a) is visible which will degrade into a cone of 51.9° (b) but rapidly acquire the maximum repose angle of 45° (c). On the right is the expected evolution of that sphere, initially releasing minor blocks (d), rapidly forming a steep talus (e), slowly evolving into a more gently sloping talus (f) and exposing the original boulder (dark grey) in the upper part of the cone.

surfaces (Figure 4A, Figure 4B) associated with blocks of a hard snowpack. Sliding of blocks in avalanches would be quite comparable to those blocks transformed into molards described for the Pink Mountain slide (Geertsema *et al.*, 2006, figure 14) and mentioned for submarine outrunners (Nissen *et al.*, 1999; De Blasio *et al.*, 2006). Therefore, a combination of flow mechanisms in these permafrost-fed avalanches is highly possible and may explain the different external characteristics observed. Sometimes, the debris will flow as a non-cohesive mass, well lubricated and/or with low-effective shear stress and thus the flow could be partially supported by the fragmentation of the permafrost body, as explained for long run-out rock/debris avalanches even in the absence of a liquid pore fluid (e.g. Davies and McSaveney, 2002). At other times, sliding will occur over a better-lubricated, lower shear strength, or more deformable surface. In the first, and the Chita slide case, with more intergranular freedom of movement, the deposit would form progressively due to a sustained flow, creating non-synchronous lobes of different character as the flow evolved. In the second case, without much differential movement, the deposit would all be emplaced synchronously, by sliding and expanding, creating flow lines and hummocky terrains (cf. Shea and Van Wyk de Vries, 2008; Dufresne and Davies, 2009). The second case would explain the conspicuous flow lines of the Sherman slide (Marangunic and Bull, 1968), where sliding and a very low rate between the vertical and horizontal travel distances of the landslide, and high-excess travel distance (Table 1) would be facilitated by a layer of snow inhibiting mixing of material along those flow lines, instead of the proposed 'air cushion' hypothesis (Shreve, 1966). However, the xenolithological debris cones described as molards would form afterwards, as suggested here, and not as part of the late flow effects of fluid escape. Although there are insufficient observations to confirm this, those sliding flows may not generate outrunners, unlike non-cohesive block and debris flows.

The Origin of Molards

The presence of molards beyond the edges of the Chita landslide, overlying a clean and vegetated alluvial plain (Figures 2 and 4) without disrupting the surrounding vegetation and partially overlying it, rules out an origin by finer debris accumulation around boulder cores as the flow ends (Hypothesis 1, Goguel and Pachoud, 1972) because the flow never reached that place. It also rules out the interpretation of cones formed by ground vibration (Hypothesis 2, Cassie *et al.*, 1988) as there is no trace of any flow material around the detached cones. For the same reason, the hypotheses that they were formed by flow differential velocities (Hypothesis 3, Dufresne and Davies, 2009) or by the release of excess pore pressure of the slide (Hypothesis 4, Shreve, 1966; Evans *et al.*, 2009) are also discounted. The fifth hypothesis of molards generated by cohesion caused by friction between two layers moving at different velocities (Shea and Van Wyk de Vries, 2008) does not apply either for those detached molards produced by outrunners.

What is clear is that the role of permafrost in molard generation is the ability of ice to cement a bouldery debris. Therefore, ice-depleted permafrost would not generate molards. Conversely, in some cases, other types of variable cohesion could create features similar to molards, although it is suggested that they could be rare, and probably not related to coarse-grained debris, as once stones are released, they will work crushing non-cemented boulders. In flows dominantly fed by fine-grained material such as sand or mud, original or secondary cohesion as that described by Shea and Van Wyk de Vries (2008) may be enough to produce molards. It is possible that molards described and portrayed for the Sale Mountain slide that was sourced by a thick, semi-cohesive loess succession (Zhang *et al.*, 2002) had its origin related to secondary cohesion because slickensides were described on the sides of the cones. The revision of all areas of molard occurrence using Gruber's (2012) global permafrost model (Table 1) also suggests that the Sale Mountain molards were not associated with permafrost. The same model applied to the Frank slide does not clearly show the existence of permafrost today. However, as the Frank slide occurred in 1903 (Cruden *et al.*, 2003) and on a north-facing slope, without too much delay after the end of the Little Ice Age, it could have been produced by relict permafrost degradation still present after that climate change.

If rubble and heterogeneous soils are always considered as source material, most debris avalanche components would not evolve towards cohesion, but rather towards fragmentation. The interpretation of Brideau *et al.* (2010), supported by the observed ice cement of boulders, is the only one that fits the facts described for the Chita molards. Thus, it is suggested that in most cases this is the most likely explanation because most typical molards are described in association with periglacial regimes.

The importance of understanding molard origin is twofold, due to its possible relation to risks associated with landslides that involve permafrost. The primary risk is the direct effect of the landslide emplacement. There are cases such as the Khait landslide that caused thousands of casualties and revealed numerous molards (Evans *et al.*, 2009). This slide could be related to permafrost, but there is no detailed study of the source material nor a unified interpretation of molards. A secondary risk is the formation of ice core dams by avalanche deposits. There are many rock glaciers in the Andes containing more than 90 per cent ice in their cores (Gestión Ambiental Consultores (GAC), 2012), and thus their failure and subsequent river damming would produce unstable situations that might lead to catastrophic outburst floods, in a way comparable to those jokülhlaups produced by glacier obstruction of streams (cf. Paterson, 1994), due to the possibility of floating part of the dam. Piping of the avalanche dam due to melting ice would also add a risk for rapid dam collapse.

CONCLUSIONS

The Chita landslide provides new evidence for the interpretation of molards observed within glacial and periglacial mountain environments. This landslide evolved into a granular flow, comparable to a debris avalanche. The independent movement of clastic components is proven by the existence of outrunners, today transformed into isolated molards detached from the main deposit. Outrunners are thought to have rolled or slid over snow, and formed many isolated cones located up to 100 m from the flow tip, suggesting that individual boulders had different momenta during the flow and when they were leaving lobe fronts. Outrunners are a key element to rule out several previous hypotheses for molard formation.

Close inspection of the original boulder composition (sometimes matrix and cement-free gravel) indicates that disaggregation during transport could only be prevented by ice cementation, which is also indicated by the fact that avalanche material was supplied by the failure of the lower part of an active rock glacier, which locally has a core of ice-bearing permafrost. Thus, it is estimated that the Chita debris avalanche was sourced in *c*. 80 per cent from ice-cemented permafrost, explaining why it is fully blanketed by molards. As permafrost boulders were brought to lower altitudes and less protected places, they rapidly lost their ice and degraded into the enigmatic molards.

Cone shape is proposed to depend on the original boulder shape and degradation rate, the latter being influenced by the boulder composition and thermal regime where molards rest. The degradation process creates the micro-talus whose formative colluvial process explains the observed grain size bimodality (coarse-grained boulder core and a finer-grained sediment apron). Molard presence may elucidate the origin of failures, the transport mode of the involved landslide and dating of the flow using the state of cone degradation or dating of the first layers of the micro-talus. While molards may indicate the loss of ground ice of the local permafrost and hence creating a primary natural risk, a secondary risk of damming streams could also be a matter of concern, since a large proportion of ice and snow could be involved in these failures.

ACKNOWLEDGEMENTS

Alicia Bonvechi (SEGEMAR) provided pre-Chita slide aerial photographs, and Dr Gabriel Guevara, the field photographs of the Altares slide molards. The Slopes Consortium of the University of Aberdeen (UK) helped with the logistics, and the Humboldt Foundation (Germany) helped with the laboratory work. Excellent reviews provided by *PPP*, Sam McColl, an anonymous reviewer and the Editor, Prof. Murton, improved the original version of this paper immensely.

REFERENCES

Blikra LH, Nemec W. 1998. Postglacial colluvium in western Norway: Depositional processes, facies and palaeoclimatic record. *Sedimentology* **45**: 909–959.

Brideau MA, Stead D, Lipovsky P, Jaboyedoff M, Hopkinson C, Demuth M, Barlow J, Evans S, Delaney K. 2010. Preliminary description and slope stability analyses of the 2008 Little Salmon Lake and 2007 Mt. Steele landslides, Yukon. In *Yukon Exploration and Geology 2009*, MacFarlane KE, Weston LH, Blackburn LR (eds). Yukon Geological Survey: Whitehorse, Canada; 119–133.

Cassie JW, Van Gassen W, Cruden DM. 1988. Laboratory analogue of the formation of molards, cones of rock-avalanche debris. *Geology* **16**: 735–738.

Clague JJ, Huggel C, Korup O, McGuire B. 2012. Climate change and hazardous processes in high mountains. *Revista de la Asociación Geológica Argentina* **69**: 328–338.

Croce F. 2006. Estudio geofísico e importancia hídrica de glaciares cubiertos y de rocas de la cuenca del arroyo Agua Negra. PhD thesis, Dept. Geofísica, Biblioteca FCEFyN, Universidad Nacional de San Juan, Argentina, 354

Croce F, Milana JP. 2002. Internal Structure and behaviour of a rock glacier in the Arid Andes of Argentina. *Permafrost and Periglacial Processes* **13**: 289–299. DOI:10.1002/ppp.431

Cruden DM, Langenberg W, Paulen R. 2003. Geology of the Frank Slide and southwestern Alberta. Edmonton Geological Society, Field Guide, 34

Davies TRH, McSaveney MJ. 2002. Dynamic simulation of the motion of fragmenting rock avalanches. *Canadian Geotechnical Journal* **39**: 789–798.

De Blasio FV, Engvik LE, Elverhøi A. 2006. Sliding of outrunner blocks from submarine landslides. *Geophysical Research Letters* **33**: L06614. DOI:10.1029/2005GL025165

Deline P, Ravanel L. 2011. Case studies in the European Alps – rockfalls in the Mont Blanc massif, French-Italian Alps. In *Thermal and Geomorphic Permafrost Response to Present and Future Climate Change in the European Alps*, Kellerer-Pirklbauer A, Lieb G, Schoeneich P, Deline P, Pogliotti P (eds). PermaNET Final Report Action 5.3. http://www.permanet-alpinespace.eu [November 2015].

Dufresne A, Davies TR. 2009. Longitudinal ridges in mass movement deposits. *Geomorphology* **105**(3-4): 171–181.

Duguay C, Zhang T, Leverington DW, Romanovsky VE. 2005. Satellite remote sensing of permafrost and seasonally frozen ground. In *Remote Sensing of Northern Hydrology*. AGU Geophysical Monograph Series. ADRA: Graz; **163**. DOI: 10.1029/163GM06

Evans SG, Roberts NJ, Ischuk A, Delaney KB, Morozova GS, Tutubalina O. 2009. Landslides triggered by the 1949 Khait earthquake, Tajikistan and associated loss of life. *Engineering Geology* **109**(3-4): 195–212.

Gestión Ambiental Consultores (GAC). 2012. Línea de base: medio fisico: glaciares. In *EIA Proyecto expansión Andina 244, CODELCO, Cap. 2.4.7*. http://seia.sea.gob.cl/ Expediente 6044819 [April 2015].

Geertsema M, Hungr O, Schwab JW, Evans SG. 2006. A large rockslide-debris avalanche in cohesive soil at Pink Mountain, northeastern British Columbia, Canada. *Engineering Geology* **83**(1–3): 64–75. DOI: 10.1016/j.enggeo.2005.06.025

Goguel J, Pachoud A. 1972. Géologie et dynamique de l'écroulement du Mount Granier, dans le Massif de Chartreuse, en novembre 1248. *Bulletin du Bureau de Recherche Géologique et Minière* **1**: 29–38.

Gruber S. 2012. Derivation and analysis of a high-resolution estimate of global permafrost zonation. *The Cryosphere* **6**: 221–233. DOI: 10.5194/tc-6-221-2012

Hungr O. 1990. Mobility of rock avalanches. Report of the National Research Institute for Earth Science and Disaster Prevention, Tsukuba, Japan, **46**: 11–20.

Intergovernmental Panel on Climate Change. 2007. Climate Change 2007: Synthesis Report **1**: 73. http://www.ipcc.ch/ [April 2015].

Jun-Jie W, Di Z, Yue L, Hui-Bo W. 2013. Angle of repose of landslide debris deposits induced by 2008 Sichuan Earthquake. *Engineering Geology* **156**: 103–110.

Kellerer-Pirklbauer A, Lieb G, Schoeneich P, Deline P, Pogliotti P (eds). 2011. *Thermal and Geomorphic Permafrost Response to Present and Future Climate Change in the European Alps*. PermaNET Final Report Action 5.3. http://www.permanet-alpinespace.eu [April 2015].

Kleinhans MG, Markies H, de Vet SJ, Veld AC, Postema FN. 2011. Static and dynamic angles of repose in loose granular materials under reduced gravity. *Journal of Geophysical Research* **116**: E11004. DOI:10.1029/2011JE003865

Kull C, Grosjean M, Veit H. 2002. Modeling Modern and Late Pleistocene glacioclimatological conditions in the North Chilean Andes (29 S–30 S). *Climate Change* **52**: 359–381.

Lachenbruch AH, Sass JH, Marshall BV, Moses TH. 1982. Permafrost, heat flow, and the geothermal regime at Prudhoe Bay, Alaska. *Journal of Geophysical Research* **87**(Bll): 9301–9316.

Luckman BH, Villalba R. 2001. Assessing the synchroneity of glacier fluctuations in the Western Cordillera of the Americas during the last millennium. In *Interhemispheric climate linkages*, Markgraf V (ed). Academic Press: San Diego; 119–140.

Marangunic C, Bull C. 1968. The landslide on the Sherman Glacier. In *The Great Alaska Earthquake of 1964*, (Hydrology Volume). Committee on the Alaska Earthquake (ed). National Academy of Science: Washington. Pub. N 1603: 383–394.

McConnell RG, Brock RW. 1904. Report on the great landslide at Frank, Alberta, 1903. Dominion of Canada, Department of the Interior, Annual Report, 1903, part VIII: 3–17.

Milana JP. 2006. Linea base de la criosfera. In EIA Proyecto Pascua-Lama. http://seia.sea.gob.cl, Expte 1048260, Addenda, 6316_2005_11_13_OD/Anexo III-A.pdf [April 2015].

Milana JP. 2011. *Hielo y Desierto – Los Glaciares Aridos de San Juan*, Elite Impresiones (ed). San Juan; 192.

Milana JP, Guell A. 2008. Las propiedades mecánicas del permafrost de Glaciares de Roca en relación a su origen y contenido de hielo, Sistema El Tapado, IV Región. *Revista de la Asociación Geológica Argentina* **63**(3): 310–325.

Minetti JL, Vargas WM. 1998. Trends and jumps in the annual precipitation in South America, south of 15S. *Atmosfera* **11**: 205–221.

Minetti JL, Vargas WM, Poblete AG, Acuña LR, Casagrande G. 2003. Non-linear trends and low frequency oscillations in annual precipitation over Argentina and Chile, 1931-1999. *Atmosfera* **16**: 119–135.

Nissen SE, Haskell NL, Steiner CT, Cotterill KL. 1999. Debris flow outrunner blocks, glide tracks, and pressure ridges identified on the Nigerian continental slope using 3-D seismic coherency. *Leading Edge* **18**: 595–599.

Paterson WSB. 1994. *The Physics of Glaciers*, 3rd edition. Oxford: Pergamon; 480.

Reineck HE, Singh IB. 1979. *Depositional Sedimentary Environments*, 2nd edition. Berlin: Springer-Verlag; 551.

Rivera A, Casassa G, Acuña C, Vieira R. 2000. Recent glacier variations and snow line changes in central Chile. In *Proceedings Sixth International Conference on Southern Hemisphere Meteorology and Oceanography, Santiago Chile*; 274–275.

Rutllant J, Fuenzalida H. 1991. Synoptic aspects of the central Chile rainfall variability associated with the Southern Oscillation. *International Journal of Climatology* **11**: 63–76.

Schrott L. 1991. Global solar radiation, soil temperature and permafrost in the Central Andes, Argentina: a progress report. *Permafrost and Periglacial Processes* **2**: 59–66.

Shea T, Van Wyk de Vries B. 2008. Structural analysis and analogue modeling of the kinemetics and dynamics of rockslide avalanches. *Geosphere* **4**(4): 657–686.

Shreve RL. 1966. Sherman Landslide, Alaska. *Science* **154**: 1639–1643.

Shreve RL. 1968. Sherman landslide. In *The Great Alaska Earthquake of 1964 (Hydrology Volume)*. National Academy of Science. Pub. N **1603**: 395–401.

Siebe C, Komorowski JC, Sheridan MF. 1992. Morphology and emplacement of an unusual debris-avalanche deposit at Jocotitlán volcano, Central Mexico. *Bulletin of Volcanology* **54**: 573–589.

Strom AL, Abdrakhmatov KE. 2009. Rockslides and rock avalanches of the Kokomeren river basin (Central Tien Shan). ICL summer school on rockslides and related phenomena guidebook. http://www.iclhq.org/Summer_School_Guidebook-2009.pdf [April 2015].

Trombotto D, Borzotta E. 2009. Indicators of present global warming through changes in active layer-thickness, estimation of thermal diffusivity and geomorphological observations in the Morenas Coloradas rockglacier, Central Andes of Mendoza, Argentina. *Cold Regions Science and Technology* **55**: 321–330.

Vuille M, Milana JP. 2007 High-latitude forcing of regional aridification along the subtropical west coast of South America. *Geophysical Research Letters* **34**: L23703. DOI: 10.1029/2007GL031899

Washburn AL. 1973. *Periglacial Processes and Environments*. Edward Arnold Publishers: London.

Xu Q, Shang Y, Van Asch T, Wang S, Zhang Z, Dong X. 2012. Observations from the large, rapid Yigong rock slide – debris avalanche, southeast Tibet. *Canadian Geotechnical Journal* **49**(5): 589–606. DOI:10.1139/t2012-021

Zhang ZY, Chen SM, Tao LJ. 2002. 1983 Sale Mountain landslide, Gansu province, China. In *Catastrophic landslides: effects, occurrence, and mechanisms,* Evans SG, Degraff JV (eds). The Geological Society of America: Boulder, CO, USA; 149–163.

Zischg A, Mair V, Lang K, Deline P, Ravanel L, Schoeneich P, Kellerer-Pirklbauer A. 2012. Consideration of permafrost and permafrost degradation in natural hazards assessment. In *Proceedings 12th Congress INTERPRAEVENT 2012 – Grenoble/France*, International Research Society (ed). Provincial Government of Carinthia Dept. 8 - Environment, Water and Nature Protection: Klagenfurt Austria; http://www.interpraevent.at [November 2015].

SUPPORTING INFORMATION

Additional supporting information may be found in the online version at the publisher's web site.